



The origin of infrared bands in nitrogen-doped Si

M. S. Potsidi^{1,*} , T. Angeletos^{1,*}, and C. A. Londos^{1,*}

¹Department of Physics, Section of Condensed Matter Physics, National and Kapodistrian University of Athens, Panepistimiopolis Zografos, 157 84 Athens, Greece

Received: 3 September 2021

Accepted: 1 December 2021

Published online:

18 February 2022

© The Author(s), under exclusive licence to Springer Science+Business Media, LLC, part of Springer Nature 2022

ABSTRACT

This work reports Fourier-transform infrared spectroscopy (FTIR) investigations on electron irradiated, nitrogen-doped Czochralski-grown silicon (Cz-Si). The study focuses mainly on the detection and thermal evolution of bands related to various nitrogen (N) and vacancy-nitrogen substitutional (VN)-related defects formed prior and after the irradiation of the material. Thus, in the first place, we refer to the presence of bands related to N impurity in the range 640–720 cm⁻¹ of IR spectra, where most VN defects are expected to give signals. Then, by following the thermal evolution of the detected IR bands and by considering the formation energies of the various N and VN defects, we discuss their possible correlation with different N or VN defects. We suggest that (i) the 650 cm⁻¹ band relates to the N_s and with the VN₁ at different temperature ranges, (ii) the 655 cm⁻¹ relates to the N_s defect, (iii) the 660 cm⁻¹ relates to the VN₁ defect, (iv) the 678 cm⁻¹ band relates to the N_i-N_s defect and the V₂N₂ defect at different temperature ranges, (v) the 684 cm⁻¹ band relates to the VN₂ defect, and (vi) the 689 cm⁻¹ band relates to the N_i, VN₁ and V₂N₂ defect at different temperature ranges.

Introduction

Point defects and impurities are always present in semiconductors due to thermodynamic reasons, but also as a result of material growth and processing. They can affect the physical properties of the materials and have a decisive role in the performance of devices. Notably, various impurities are introduced intentionally in the crystal to tailor the properties of the material for specific applications [1–4]. Enhancing

the material properties via the incorporation of impurities is one of the main purposes in the semiconductor industry. In that respect, the introduction of light impurities in silicon (Si) such as hydrogen (H), lithium (Li), carbon (C), nitrogen (N) and oxygen (O) is a common technique.

The present investigation focuses on N, which is an important light impurity in Si, studied intensively for the over 50 years. In particular, N introduction in Si material has been mainly used as a tool to improve its quality by modifying the physical properties for

Handling Editor: Kevin Jones.

Address correspondence to E-mail: mpotsidi@phys.uoa.gr; angelet@phys.uoa.gr; hlontos@phys.uoa.gr

various device applications. N shows a very strong locking on dislocations thus increasing the mechanical strength [5–7] of the wafers. This is very important for the very large-scale integration (VLSI) and ultralarge-scale integration (ULSI) technologies of Si, allowing the material to extend the range of processing steps without wafer breaking. In essence, N incorporation leads to larger wafer diameter and improves material quality as far as the requirements for wafer flatness and mechanical stability. N also enhances the ability of the oxygen precipitation process [8, 9], facilitating internal gettering procedure thus suppressing the deleterious effects of metallic contaminants. The presence of N atoms suppresses the generation of some microdefects during crystal growth, as, for instance, the A-swirls and D-defects/voids in N-doped Fz-Si [10, 11]. Additionally, N reduces the formation [12] of voids that cause degradation of Si devices and can lead to a failure of gate oxides [13]. In general, N has the tendency to interact with intrinsic defects (such as vacancies and self-interstitials) affecting the early stages of defect dynamics during Si crystal growth [12–14]. Additionally, N impacts oxygen-related defects affecting the creation of thermal donors and shallow thermal donors in Si [6, 15] and influences the electrical [6, 16] properties of Cz-Si. In irradiated silicon, N doping limits the formation of vacancy-oxygen defects (VO or A-centers), the presence of which has generally negative effects in the performance of devices [17, 18]. Furthermore, it enhances oxygen precipitate formation [19]. In summary, N affects the mechanical, electrical and optical properties [5–7, 16, 20, 21] of Si and the more we know about its behavior as an impurity the better the control of the material for device applications.

Although N belongs to the V group of the periodic table, it is an ineffective donor conversely to phosphorous (P), arsenic (As) and antimony (Sb) which are n-type dopants in Si [22]. Importantly, the solid solubility [23] of N in Si is low approaching at the melting point $4.5\text{--}10 \times 10^{15}$ atoms/cm³, which is more than two orders of magnitude less than that of O and C in Si. It has been determined [12, 24, 25] that N interacts strongly with O, C, vacancies and self-interstitials. The main families of defects in N-doped Cz-Si are nitrogen-oxygen and nitrogen-vacancies complexes. The present study focuses on the latter complexes where there are still unclear points regarding their properties and behavior. Regarding

the vacancy-nitrogen substitutional defect (VN₁), with local vibrational mode (LVM), signals in the range 663–669 cm⁻¹ have been correlated with the N residing in a substitutional position [26–30]. LVM signals at 726 and 778 cm⁻¹ have been correlated with the VN₂ complex [31]. Additionally, a LVM value at 551 cm⁻¹ has also been reported [28, 32], and values in the range 665–693 cm⁻¹ have been calculated [26, 30] for this center. Regarding the V₂N₂ complex, an LVM value at 689 cm⁻¹ has been reported [31], although a value at 653 cm⁻¹ [12] and calculated values in the range 669–694 cm⁻¹ [30] have also been cited in the literature. Thus, the picture regarding band assignments for the VN₁, VN₂, V₂N₂ and generally nitrogen-vacancy-related defects is not yet clear.

The purpose of the present study is to investigate the relation between the spectral identity and thermal evolution behavior of various nitrogen-vacancy structures in Si and contribute to their band assignment in the different temperature ranges. Importantly, these complexes have been reported [19, 33, 34] to function as precipitate nuclei and also affect the void formation in Si, a critical point for Si semiconductor industry. As a result of the low concentration of N in Si, the corresponding signals of the relative defects are quite weak. Irradiation is an efficient way to enhance the formation of nitrogen-vacancy defects. This is because during irradiation, there will be a supersaturation of vacancies and a higher number of these vacancies will be associated with N effectively increasing the concentration of the nitrogen-vacancy defects. To investigate these defects, we will employ infrared spectroscopy measurements in irradiated N-doped Si. Remarkably, only in the last few years have been made such considerable measurements [17, 31].

Experimental details

Samples cut from prepolished Cz-Si wafers were used. The N concentration given by the provider was 5×10^{14} cm⁻³. The O concentration was determined by a Fourier-transform infrared (FTIR) spectrometer using a calibration coefficient of 3.14×10^{17} cm⁻² (ASTM F 121–89 standard). The C concentration was beyond detection limit. The samples were subjected to 2 MeV electron irradiation with a fluence of 2×10^{18} cm⁻², at ~ 70 °C, using the facilities of the

Figure 1 Segment of the IR spectra in the range 640–720 cm^{-1} **a** before irradiation (as-grown sample), **b** after irradiation, **c** at 50 °C and **d** at 200 °C.

Dynamitron accelerator at Takasaki-JAERI (Japan). After the irradiation, the samples were subjected to a series of 20 min isochronal anneals up to 1200 °C in open furnaces with a step of ~ 10 °C. After each annealing step, IR spectra were recorded at room temperature (RT) employed an FTIR spectrometer (JASCO-70 plus) operated with a resolution of 1 cm^{-1} . The two phonon background absorption was subtracted from each recorded spectrum by using a Float-Zone (FZ-Si) sample of equal thickness as that of the CZ-Si sample.

Experimental results and discussion

Figure 1 shows the IR spectra in the range 640–720 cm^{-1} taken (a) before irradiation (as-grown sample), (b) after irradiation, (c) after thermal treatment at 50 °C and (d) after thermal treatment at 200 °C. Figures 2 and 3 show the IR spectra in the range 640–720 cm^{-1} after thermal treatment at characteristic temperatures in the range 300–1100 °C. In the spectrum of the as-grown material, one could immediately detect the bands at 645, 655, 660, 678, 689, 697 and 706 cm^{-1} . After irradiation, the bands at 655, 678 and 697 remain in the spectrum, the bands at 660, 689 and 706 cm^{-1} diminish, and a band at 650 cm^{-1} emerges. In an attempt to correlate the detected bands with possible candidates from the family of N_s -related defects, we have taken into account.

- i. that the high-intensity signals of N_s -related defects [29] lie in the frequency range 645–720 cm^{-1} ,
- ii. the formation energies of the various N_s -related defects as given in recent studies [26, 28–30],
- iii. that vacancies could be created in the crystal during growth, although their concentration dependence on the crystal growth parameters remains complicated [26]. Values of the order of $\sim 10^{15} \text{ cm}^{-3}$ have been proposed [35], and it is expected that if the nitrogen concentration exceeds that of the vacancy's, vacancy-nitrogen

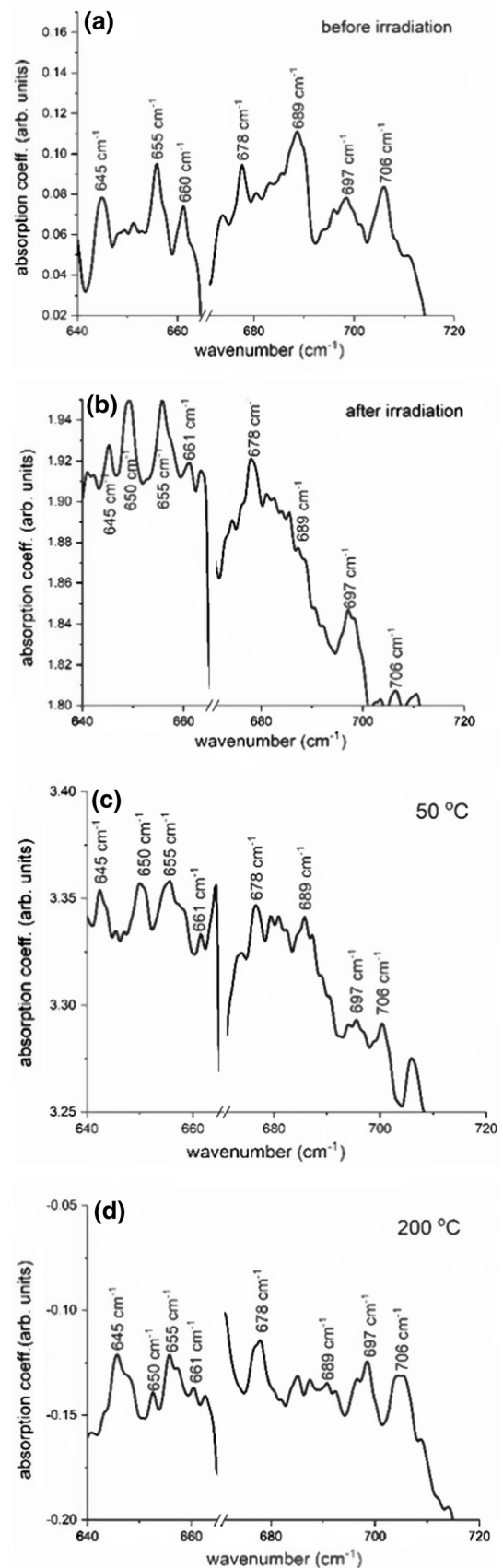


Figure 2 Segment of the IR spectra in the range 640–720 cm^{-1} after annealing at the temperatures **a** 300 °C, **b** 450 °C, **c** 550 °C, **d** 600 °C.

defects could form [26] even during growth (prior to irradiation).

- iv. all N_s -related complexes are aggregates of vacancy with nitrogen atoms and form with the addition of lattice vacancies to single nitrogen interstitial atoms (N_i) or interstitial-nitrogen pairs [26] (N_i-N_i).

In all presented spectra, the range 665–671 cm^{-1} has been removed, as it contains the relatively intense peak of CO_2 at $\sim 668 \text{ cm}^{-1}$ [36].

The 650 cm^{-1} band

The band at 650 cm^{-1} appears strong in the spectrum only after irradiation and its emergence coinciding with the decrease of the 689 cm^{-1} band possibly attributed to the N_i defect [37] (see below). Candidates for the 650 cm^{-1} band could be either the N_s defect (experimentally detected [24, 28] at 653 cm^{-1} and theoretically predicted at 637 cm^{-1} [26] and 645 cm^{-1} [30] for the C_{3v} symmetry), or the intense peak of VN_1 (theoretically predicted at 654 and 668 cm^{-1} [30]. N_s defect is formed with the addition of a vacancy to a nitrogen interstitial atom [26]. Similarly, the VN_1 defect is a complex of N_s with a vacancy [26]. Both N_s and VN_1 defects could form during irradiation, provided that the formation energies of N_s and VN_1 defects do not exceed the vacancy formation energy. The latter has been calculated for various approximations and symmetries with values ranging from 3.17 to 4.13 eV [38, 39]. It is important to notice that the experimental vacancy formation energy has been found at 4 eV [40]. The formation energy of N_s (1.96 eV [30]) is significantly lower than that of the vacancy, while the formation energy of VN_1 (3.79 eV [30] and 3.71 eV [26]) competes that of the vacancy's. Therefore, on the basis of vacancy excess in the crystal after irradiation, the formation of N_s defects seems to be prioritized energetically against the formation of the VN_1 defects, favoring the correlation of the 650 cm^{-1} band with the N_s defect. Of course, at this stage, one cannot exclude the VN_1 defect from candidacy.

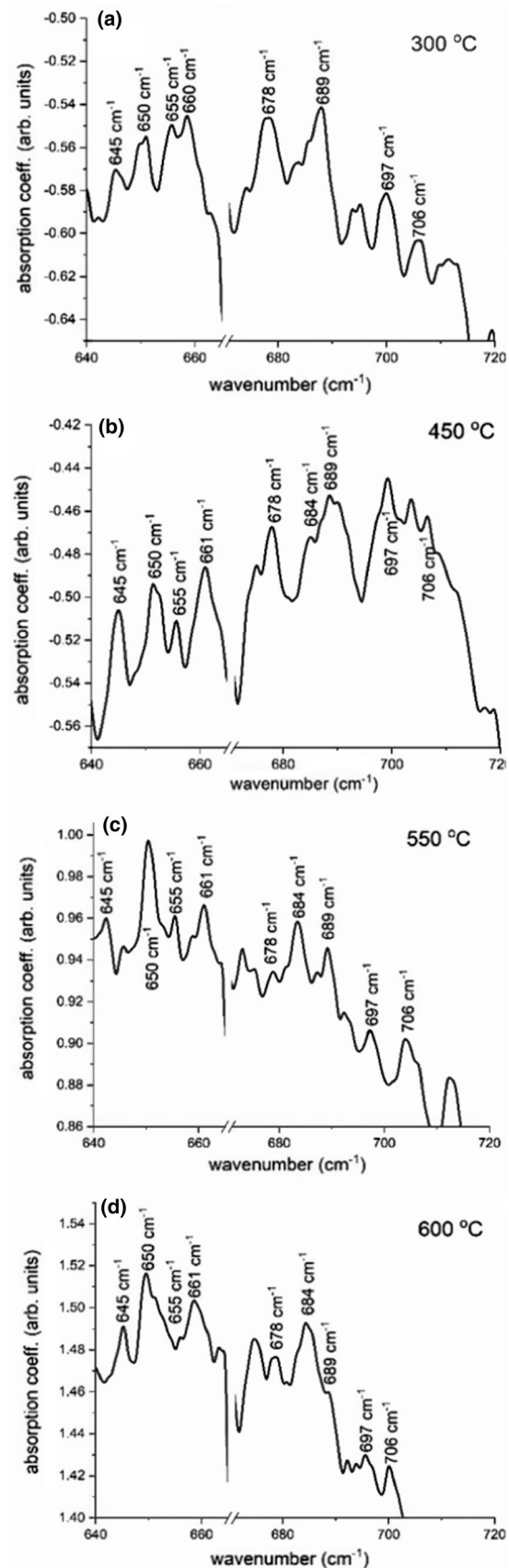


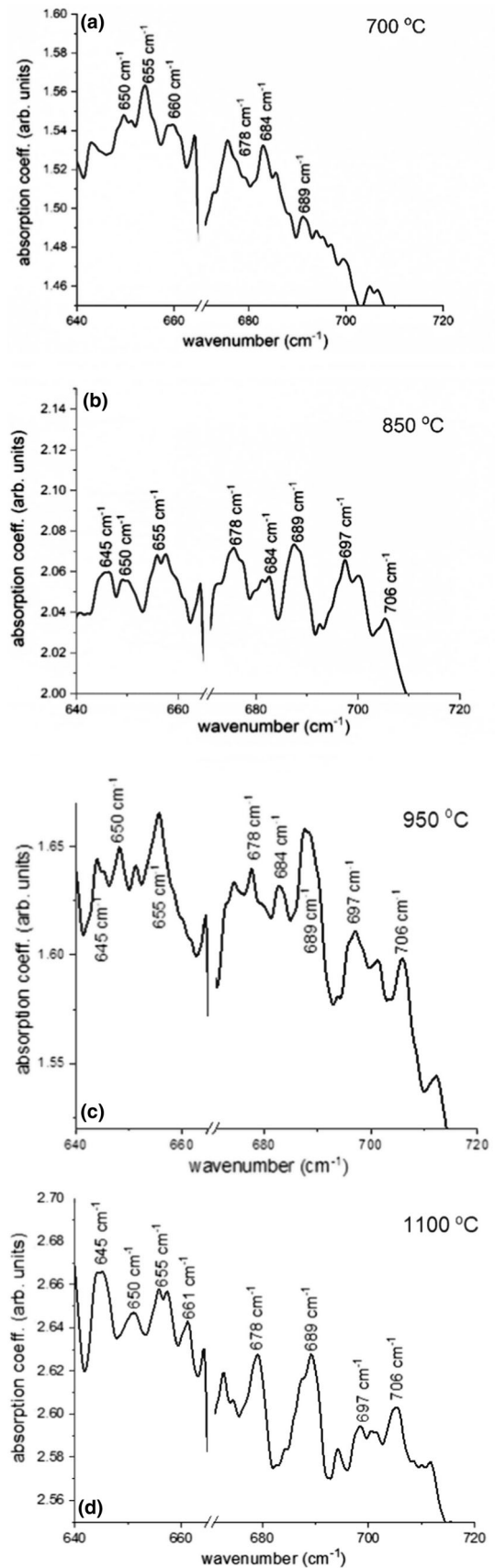
Figure 3 Segment of the IR spectra in the range 640–720 cm^{-1} after annealing at the temperatures **a** 700 °C, **b** 850 °C, **c** 950 °C, **d** 1100 °C.

Examining the thermal behavior of the 650 cm^{-1} band, we detect its disappearance around ~ 200 °C (Fig. 1), its reappearance in the range ~ 300 – 600 °C (Fig. 2). The band finally anneals out just above ~ 600 °C (Fig. 3). If one assumes that the 650 cm^{-1} band relates to the N_s defect up to ~ 200 °C, then by capturing vacancies in the range 300–600 °C (sources of these vacancies are vacancy-oxygen defects [31, 41] or vacancy-related clusters [9, 42]) could transform to VN_1 defects. Notably, the VN_1 defect is expected to form at higher formation energies of 3.79 eV [30] (or 3.71 eV [26]) and its highest intensity LVM band corresponding to a C_{3v} symmetry. In this symmetry for the VN_1 defect, a calculated LVM frequency value at 654 cm^{-1} has been reported [30]. An additional argument on the connection of the 650 cm^{-1} band with the VN_1 defect in the range 300–600 °C was given by Stein [28]. In that work, it was stated that the loss of the N_s defect after a 350 °C annealing and the increase of the SL6 and SL7 EPR signals could relate. Goss et al. [26] report that the latter EPR signals possibly relate to the of VN_1 and VN_2 defects, respectively.

Thus, we suggest that the 650 cm^{-1} band possibly correlates with the N_s defect up to ~ 200 °C and with the VN_1 defect in the T range 300–600 °C.

The 655 cm^{-1} band

The band at 655 cm^{-1} appears in the spectra of the as-grown sample as well as of the as-irradiated sample exhibiting similar intensities in both spectra (Fig. 1). Its signal progressively decays toward ~ 600 °C and increases again from ~ 850 °C onwards, staying detectable up to 1100 °C (Figs. 2 and 3). For the 655 cm^{-1} band, possible candidates are (i) the N_s defect (as discussed above) or (ii) the VN_1 defect (theoretically predicted [30] at 654 cm^{-1} for the C_{3v} symmetry and at 664 and 673 cm^{-1} for the C_s symmetry). If we assume that the 689 cm^{-1} band belongs to the N_i defect [37] (see below), then one could correlate the 655 cm^{-1} band, which is of similar intensity with the 689 cm^{-1} band in the as-grown sample (Fig. 1), with the N_s defect. At first, the two bands are expected to have equal concentrations in equilibrium



conditions [26] (Fig. 1). It is worth noting that although the vacancy concentration during crystal growth is expected around $\sim 10^{12} \text{ cm}^{-3}$, values at $\sim 10^{15} \text{ cm}^{-3}$ have also been reported [26], making the formation of the nitrogen-vacancy-related N_s defect possible even during crystal growth conditions [26]. Regarding now, a possible connection of the 655 cm^{-1} band with the VN_1 defect this seems less possible, since the VN_1 defect has been reported to increase after annealing at $350 \text{ }^\circ\text{C}$ [37] or form after annealing in the range $\sim 380\text{--}450 \text{ }^\circ\text{C}$ [43], a thermal behavior opposite to that shown by our 655 cm^{-1} band.

We notice that increase of the 655 cm^{-1} above $\sim 600\text{--}650 \text{ }^\circ\text{C}$ might indicate a dissociation of existing VN_1 defects in the crystal into V and N_s . Similar arguments have been stated [31] for the case of the dissociation of irradiation-induced defects after annealing at $600 \text{ }^\circ\text{C}$ and their return to $N_i\text{--}N_i$ defects.

Thus, we suggest that the 655 cm^{-1} band possibly correlates with the N_s defect.

The 678 cm^{-1} band

The 678 cm^{-1} band appears in the as-grown sample and shows thermal stability up to $\sim 450 \text{ }^\circ\text{C}$ (Fig. 2), after which temperature disappears and reemerges at $\sim 800\text{--}850 \text{ }^\circ\text{C}$ further existing up to $1100 \text{ }^\circ\text{C}$ (Fig. 3). This behavior points toward either different originations of this band in these two temperature ranges or a reformation upon dissociation of other defects. In the discussion below, we examine and consider the evolution of the 678 cm^{-1} band at two temperature ranges.

In the T range from growth to $\sim 450 \text{ }^\circ\text{C}$

Possible candidates are the $N_s\text{--}N_s$ defect with LVM frequency values at 678 cm^{-1} [30] and 668.6 cm^{-1} [26]. The $N_s\text{--}N_i$ defect with reported LVM line at 672.8 cm^{-1} [26], as well as the VN_1 defect with calculated LVM frequency at 668 cm^{-1} [30]. The intensity of our 678 cm^{-1} band as it appears in our spectra remains unaffected by vacancy concentration enhancement during irradiation (Fig. 1). Considering the relatively low formation energy of the $N_s\text{--}N_s$ defect (0.9 eV [30]) and its reported stability due to the closed shell structure [30], at a first attempt, one could attribute our 678 cm^{-1} band to the $N_s\text{--}N_s$ defect. This connection, however, contradicts Goss

et al. [26] reporting on the $N_s\text{--}N_s$ formation. The same authors [26] report on the possibility that $N_i\text{--}N_s$ could form during nonequilibrium cooling down conditions from $1400 \text{ }^\circ\text{C}$ crystal growth if vacancy concentration reaches values $\sim 10^{15} \text{ cm}^{-3}$. Also, the reported disappearance of the $N_i\text{--}N_s$ defect around $\sim 400 \text{ }^\circ\text{C}$ [26], which agrees well with our 678 cm^{-1} defect observed decay at $\sim 450 \text{ }^\circ\text{C}$, is a further supporting argument for the latter correlation.

On the other hand, a linking with the VN_1 defect seems less favored before irradiation and up to $450 \text{ }^\circ\text{C}$, if one considers (i) the higher number of vacancies needed for a N_i defect to gradually end up to VN_1 defect (compared to the one vacancy needed for N_i pair to produce $N_i\text{--}N_s$ [26]), (ii) the higher formation energy of the VN_1 defect (3.79 [30] and 3.71 [26] eV) in relation to that of the $N_i\text{--}N_s$ formation energy (2.51 eV [29]) and (iii) the observation that the VN_1 SL6 EPR signal increases after annealing [43] at $\sim 400 \text{ }^\circ\text{C}$, while our 678 cm^{-1} band decreases after annealing around this temperature. For the above reasons, we propose that the $N_i\text{--}N_s$ defect best meets the criteria for the connection with the 678 cm^{-1} band in the range up to $\sim 450 \text{ }^\circ\text{C}$.

In the T range $800\text{--}1100 \text{ }^\circ\text{C}$

The band at 678 cm^{-1} reemerges above $\sim 800 \text{ }^\circ\text{C}$ but with lower intensity (Fig. 3). The reappearance of this band could possibly indicate either (i) the formation of higher-order vacancy aggregates with existing nitrogen defects or (ii) the dissociation of existing nitrogen VN defects into their components. Regarding the former case, such higher-order VN defects could be the V_2N_2 defects with reported LVM bands [30] at 673 cm^{-1} , as well as numerous other bands in the 678 cm^{-1} vicinity [30]. The existence of V_2N_2 defects has indeed been reported at elevated temperatures [44]. The vacancies needed for the formation of those higher-order nitrogen-vacancy defects could be provided by the actual dissociation of the various multivacancy-multioxygen (V_nO_m) defects at the temperature range above $600 \text{ }^\circ\text{C}$ [45]. We must note that oxygen precipitates that form in the crystal [46] are known to emit self-interstitials or attract vacancies in the course of their formation, in order to accommodate the volume expansion in the precipitate area [47]. The fact that precipitates form at a relatively lower temperature ($\sim 600 \text{ }^\circ\text{C}$, (Fig. 4)) in

our doped samples is an indication of release of vacancies due to the dissociation of V_nO_m defects.

In relation now, to the latter case, the onset of the 678 cm^{-1} band possibly correlates with the reformation of N_i-N_s defect (see above) due possibly to the dissociation of existing VN defects in the crystal (for example, one may consider the dissociation of VN_2 into V and N_i-N_s). A similar phenomenon has been reported by Inoue et. al. [31] in relation to a possible return of irradiation-induced nitrogen defects to N_i-N_i defects after annealing at $600\text{ }^\circ\text{C}$. Notably, in this case, also, the vacancies released by this dissociation could also contribute to the formation of additional oxygen precipitates at lower temperatures.

Thus, we suggest that the 678 cm^{-1} band possibly correlates with the N_i-N_s defect up to $\sim 450\text{ }^\circ\text{C}$. However, in the range $800\text{--}1100\text{ }^\circ\text{C}$, the picture is not clear and two possibilities exist: In this range, the defect may correlate either with the V_2N_2 defect or with the N_i-N_s defect.

The 689 cm^{-1} band

The band at 689 cm^{-1} exists in the as-grown silicon samples and decreases after irradiation (Fig. 1). Commenting on its thermal behavior, one could highlight three stages: i) a decrease occurring around $200\text{ }^\circ\text{C}$, ii) an onset at $\sim 300\text{--}450\text{ }^\circ\text{C}$ and a further decrease at $\sim 600\text{ }^\circ\text{C}$ and iii) a second increase at $\sim 800\text{--}850\text{ }^\circ\text{C}$. The band continues to exist further up to $\sim 1100\text{ }^\circ\text{C}$. These observations along with consideration of the formation energies of the VN_1 (3.79 [30] eV, 3.71 [26] eV), VN_2 (2.71 [30] eV, 3.42 [26] eV), VN_3 (2.45 eV [30]) and V_2N_2 defects (5.27 eV [30],

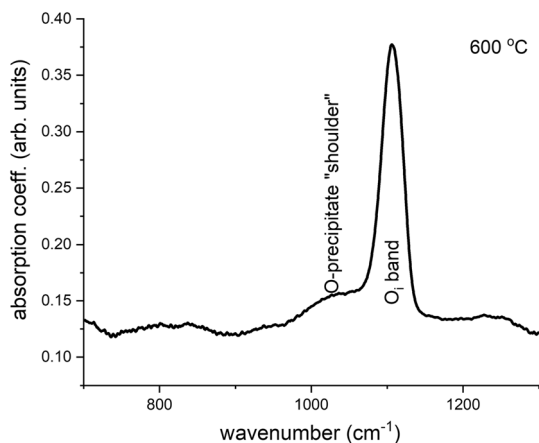


Figure 4 The 1107 cm^{-1} oxygen interstitial LVM band neighborhood at $\sim 600\text{ }^\circ\text{C}$.

5.08 eV [26]) led us to discuss different origins of the 689 cm^{-1} band in the three different temperature ranges that is i) from growth to $\sim 200\text{ }^\circ\text{C}$, ii) from ~ 300 to $600\text{ }^\circ\text{C}$ and iii) from ~ 800 to $1100\text{ }^\circ\text{C}$.

In the T range from growth to $\sim 200\text{ }^\circ\text{C}$

In a non-irradiated crystal where vacancies could form but a supersaturation environment is less favored compared to irradiated material, N_i and N_i pairs, both of which are not vacancy-related, are expected to form [26]. The N_i pair is the dominant defect in nitrogen implanted silicon [26] with a formation energy of $\sim -0.77\text{ eV}$ [29], while the formation energy of N_i defect is 2.07 eV [29]. Both values are significantly lower than the vacancy formation energy value. This has been calculated for various approximations and symmetries to range [38, 39] from 3.17 to 4.13 eV and has been reported experimentally at 4 eV [40]. The strong appearance of the band at 689 cm^{-1} prior to irradiation is a first indication of a nitrogen interstitial-related defect rather than a nitrogen substitutional one. In fact, as the N_s -related defect formation presupposes the presence of vacancies in the crystal, the significantly lower formation energy of the N_i and N_i pair defects compared to that of the vacancies supports the above correlation. Indeed, the band has been previously correlated with the N_i defect [37]. The observed decrease of the 689 cm^{-1} band in the spectra along with the simultaneous appearance of the 650 cm^{-1} band of N_s defect after irradiation as discussed above stands for the above correlation. In contrast, the low formation energy of the N_s-N_s defect (0.9 eV [30]) cannot exclude a possible correlation of our 689 cm^{-1} band with the previously theoretically derived 685 cm^{-1} N_s-N_s band [30]. However, the observed decrease before $\sim 200\text{ }^\circ\text{C}$ in our experiment does not agree with the reported stability of the N_s-N_s defect [30].

In the T range $300\text{--}600\text{ }^\circ\text{C}$

The anneal out of various multivacancy defects [9] as V_2 , V_3 , V_4 , V_5 , as well as the VO and VO_2 defects [41], could provide additional vacancies in the temperature range $\sim 300\text{--}450\text{ }^\circ\text{C}$. A reaction of these vacancies with nitrogen may lead to the formation of vacancy- N_s -related defects. Moreover, we notice the following: (i) It is known [28] that after annealing at $\sim 350\text{ }^\circ\text{C}$, a band at 687 cm^{-1} arises in the IR

spectra coinciding with the annealing out of the 653 cm^{-1} N_s band and (ii) the annealing at $\sim 380\text{--}450\text{ }^\circ\text{C}$ of samples containing SL5 (N_s) centers results in the formation of two other N centers (SL6 and SL7 [43]). Remarkably, in the above report [28], the 687 cm^{-1} band has been connected with the SL6 and SL7 EPR signals [28, 43]. These EPR signals have been possibly related [26] to the VN_1 and VN_2 defects, respectively. Platonenko et al. [30] also report on a VN_2 band at 688 cm^{-1} . Similarly, it has also been stated [31] that an experimental band at 689 cm^{-1} was intense after annealing at $400\text{ }^\circ\text{C}$, but weak at 200 and $600\text{ }^\circ\text{C}$, a behavior similar to that of our experiment. This band was, however, correlated with the V_2N_2 defect [31]. Therefore, main possible candidates for the 689 cm^{-1} band in this temperature range are either the VN_1 and VN_2 defects [26] or the V_2N_2 defects [31]. In our opinion, the latter assignment is less favored, due to its relatively higher formation energy of V_2N_2 defect (5.27 eV [30], 5.08 eV [26]) than that of the VN_1 (3.79 eV [30], 3.71 eV [26]) and VN_2 (2.71 eV [30], 3.42 eV [26]) defects. Finally, for the consistency of the analysis, we cannot leave out the VN_3 defect from possible candidacy for the 689 cm^{-1} band in this temperature range, with reported formation energy of 2.45 eV and LVM band calculated around 690 cm^{-1} [30].

In the T range $\sim 800\text{--}1100\text{ }^\circ\text{C}$

The reappearance of the 689 cm^{-1} band above $\sim 800\text{--}850\text{ }^\circ\text{C}$ and its existence up to $\sim 1100\text{ }^\circ\text{C}$ may suggest that at elevated temperatures, the VN_2 (or VN_1) transforms into V_2N_2 by capturing another vacancy. The V_2N_2 has calculated LVM frequency value at 687 cm^{-1} [30]. It has also been reported experimentally at 689 cm^{-1} by Inoue et al. [31], although these authors attribute this band to the V_2N_2 defect at lower temperatures than ours. We notice that the transformation of the VN_2 to the V_2N_2 defect and the existence of the latter at elevated temperatures has been reported previously [44]. The vacancies needed for the latter transformation could be provided by possible dissociation of V_nO_m defects [45] at elevated temperatures above $600\text{ }^\circ\text{C}$ or even by the dissociation of existing nitrogen-vacancy-related defects [31]. Lastly, one could expect the formation of V_2N_2 defects to occur at higher formation energies (5.27 eV [30], 5.08 eV [26]) than that of the VN_1 (3.79 eV [30], 3.71 eV [26]) and VN_2 (2.71 eV [30],

3.42 eV [26]), supporting that the formation of the V_2N_2 defects may be aggregates of vacancies with the VN_1 or the VN_2 defects. Therefore, it is logical to correlate the reemergence of our 689 cm^{-1} band with the formation of the V_2N_2 defect in this temperature range.

At this point, it is important to notice that V_2N_2 defects can exist at temperatures of void aggregation. This shows that their formation can affect the concentration or the diffusibility of the vacancies [44]. Based on this, we think that further studies on this defect could shed new light on the general formation of all vacancy-nitrogen-related defects in irradiated silicon.

The band at 684 cm^{-1}

Carefully analyzing the IR spectra in the temperature range $450\text{--}850\text{ }^\circ\text{C}$, one could point out the appearance of a band at 684 cm^{-1} , which rises upon the decay of the 689 and 678 cm^{-1} bands in the range $450\text{--}600\text{ }^\circ\text{C}$ (Fig. 2). At first, we attempt to correlate this band with a vacancy-nitrogen defect, considering the lower formation energies of the VN_1 , VN_2 , VN_3 compared to those of the V_2N_2 centers [26, 30]. These have been calculated as 3.79 [30] and 3.71 [26] eV for the VN_1 , 2.71 [30] and 3.42 [26] eV for the VN_2 , 2.45 [30] eV for the VN_3 and 5.27 [30] and 5.08 [26] eV for the V_2N_2 , respectively. The above values suggest that the VN_1 , VN_2 and VN_3 defects meet the criteria to form once vacancies exist in the crystal, though this does not occur for the V_2N_2 , having a much higher formation energy. Thus, in terms of formation energies, the appearance of the 684 cm^{-1} band at this relatively narrow temperature range could be related to the VN_1 , VN_2 or VN_3 defects, all of which have calculated LVM values [26, 30] in the 684 cm^{-1} neighborhood.

On the other hand, the onset of the 684 cm^{-1} band coincides with the formation of oxygen precipitates in the crystal at $\sim 600\text{ }^\circ\text{C}$. This temperature is lower compared to that in an undoped crystal [46, 47] and a possible explanation could be that the V_2N_2 defects that form at these temperatures act as nuclei for oxygen precipitates [48, 49]. Following this suggestion, one could attribute the 684 cm^{-1} band to the presence of V_2N_2 defects, as well.

Among all the above defect structures, the most possible candidates for our experimental 684 cm^{-1} band seem to be either the VN_2 structure in the C_2 symmetry [30], with a calculated value at 683 cm^{-1} or

the VN_3 structure in the C_{3v} symmetry [30] with a calculated value at 687 cm^{-1} . Notably, the latter two bands have similar and relatively high intensities [30].

The 660 cm^{-1} band

The band appears before irradiation (Fig. 1) and disappears after irradiation (Fig. 1), and it reappears with increasing intensity after annealing at $300\text{ }^\circ\text{C}$ (Fig. 2). It finally decays around $\sim 600\text{ }^\circ\text{C}$ (Fig. 2). Its thermal behavior resembles that of the 655 cm^{-1} and 689 cm^{-1} bands in the range $300\text{--}600\text{ }^\circ\text{C}$, discussed above, correlated with the VN_1 defect in this temperature range. Therefore, one reasonably could also correlate the 660 cm^{-1} band with the VN_1 defect. Importantly, Platonenko et al. [30] have also calculated a band at 664 cm^{-1} , of relatively high intensity corresponding to the C_s symmetry of the VN_1 defect.

A final comment: N in Si forms various families of defects, important among them are the vacancy-nitrogen defects which appear in all temperature ranges. Most of them are produced during growth but some after irradiation. However, their properties are not completely known and understood in comparison with the vacancy-oxygen family of defects which are dominant in irradiated Si. Vacancy-oxygen family has been studied intensively and extensively by electrical, magnetic, optical and structural methods [41, 50–53] using numerous experimental techniques, for instance, electron paramagnetic resonance (EPR), infrared absorption (IR), deep level transient spectroscopy (DLTS), positron annihilation spectroscopy (PAS) and photoluminescence (PL) among them. Since vacancy-nitrogen defects affect the behavior of Si material in many ways depending on the particular application, it is important to improve the picture regarding their properties, with this being the main purpose of the present work.

Conclusions

We have investigated N-related and VN -related bands in N-doped electron irradiated Si employing FTIR measurements at room temperatures. The thermal evolution of the bands was monitored in the temperature range from room temperature up to $1100\text{ }^\circ\text{C}$. The 650 cm^{-1} forming after irradiation

possibly relates to the N_s defect. It decays around $\sim 200\text{ }^\circ\text{C}$ (as a N_s defect), reemerges at $\sim 300\text{ }^\circ\text{C}$ (as VN_1 signal possibly due N_s to VN_1 conversion) and decays at $\sim 600\text{ }^\circ\text{C}$. The 655 cm^{-1} detected before and after irradiation with the same intensity might be due to the N_s defect. It progressively decreases toward $\sim 600\text{ }^\circ\text{C}$, and it increases again and stays detectable up to $1100\text{ }^\circ\text{C}$. The reemergence could be related to the dissociation of VN_1 defects into vacancies and N_s defects.

The 660 cm^{-1} band appears weak before irradiation, is not detected up to $300\text{ }^\circ\text{C}$ and reemerges in the range $300\text{--}600\text{ }^\circ\text{C}$. It probably relates to the VN_1 defect.

The 678 cm^{-1} and 689 cm^{-1} bands form in the as-grown sample (possibly related to the N_i - N_s and N_i defects, respectively). The 689 cm^{-1} N_i band decreases at $\sim 200\text{ }^\circ\text{C}$, then by capturing vacancies could form the 689 cm^{-1} VN_1 defect at $\sim 300\text{ }^\circ\text{C}$, by capturing further vacancies at $\sim 400\text{ }^\circ\text{C}$ could convert most possibly to VN_2 giving rise to a band at $\sim 684\text{ cm}^{-1}$ in our experiment. The 684 cm^{-1} band decays at $\sim 800\text{--}850\text{ }^\circ\text{C}$, while the 689 cm^{-1} band emerges again possibly due to further capturing of vacancies by the VN_2 defects leading to the formation of V_2N_2 defects. Regarding now the 678 cm^{-1} band, it reemerges after $\sim 800\text{--}850\text{ }^\circ\text{C}$ also staying detectable at $1100\text{ }^\circ\text{C}$. We suggest that the 678 cm^{-1} band and the 689 cm^{-1} band at temperatures above $\sim 800\text{ }^\circ\text{C}$ are connected with the presence of the V_2N_2 defects in the crystal, in agreement with the recent work by Platonenko et al.³⁰ calculating the LVM frequencies for the V_2N_2 defects remarkably close to our values at 678 and 689 cm^{-1} .

Acknowledgements

T. Angeletos would like to thank A. S. Onassis Foundation for financial support for his Ph. D. thesis through scholarship (Grant No. G ZL 001-1/2015-2016).

Data availability

The data that supports the findings of this study are available from the corresponding author upon reasonable request.

Declarations

Conflict of interest All authors certify that they have no affiliations with or involvement in any organization or entity with any financial interest or non-financial interest in the subject matter or materials discussed in this manuscript.

References

- [1] Stavola M, Fowler WB (2018) Tutorial: novel properties of defects in semiconductors revealed by their vibrational spectra. *J Appl Phys* 123:161561
- [2] McCluskey MD, Janotti A (2020) Defects in semiconductors. *J Appl Phys* 127:190401
- [3] Freysoldt C, Grabowski B, Hickel T, Neugebauer J, Kresse G, Janotti A, Van de Walle C (2014) First-principles calculations for point defects in solids. *Rev Mod Phys* 86:253–305
- [4] Alkauskas A, McCluskey MD, Van de Walle C (2016) Tutorial: defects in semiconductors-combining experiment and theory. *J Appl Phys* 119:181101
- [5] Sumino K, Yonenaga I, Imai M, Abe T (1983) Effects of nitrogen on dislocation behavior and mechanical strength in silicon crystals. *J Appl Phys* 54:5016–5020
- [6] Yuan S, Yang D (2019) Nitrogen impurity in crystalline silicon. In: Yang D (ed) *Handbook of photovoltaic silicon*. Springer Nature, Berlin, p 1–31
- [7] Drabold DA, Estreicher S (Eds) (2007) *Defect theory: an armchair history*. In: *Theory of defects in semiconductors*. Springer, Berlin, p 11–27
- [8] Shimura F, Hokket RS (1986) Nitrogen effect on oxygen precipitation in Czochralski silicon. *Appl Phys Lett* 48:224–226
- [9] Pichler P (2004) Intrinsic point defects, impurities, and their diffusion in silicon. In: Selberherr S (ed) *Computational microelectronics*. Springer, NewYork, p 378–390
- [10] Von Ammon W, Sattler A, Kissinger G (2017) *Springer handbook of electronic and photonic materials (Chapter 5: defects in monocrystalline silicon)*, S. Kasap and P. Capper (Eds), p 111–132
- [11] Abe T, Harada H, Chikawa G (1983) Microdefects and impurities in dislocation-free silicon crystals, *Mater Res Soc Symposium Proc* 14:1–17
- [12] Yu X, Chen J, Ma X, Yang D (2013) Impurity engineering in Czochralski Silicon. *Mater Sci Eng R* 74:1–33
- [13] Ishii H, Oka K, Motonami K, Koyama T, Izumitani J (1996) Direct observation of crystal-originated particles on Czochralski-grown silicon wafer surface and effect on gate oxide reliability. *Jpn J Appl Phys part 2* 35:L1385–L1387
- [14] von Ammon W, Holz R, Virbulis J, Dornberger E, Schmolke R, Graff D (2001) The impact of Nitrogen on the defect aggregation in silicon. *J Crystal Growth* 226:19–30
- [15] Yang D, Que D, Sumino K (1995) Nitrogen effects on thermal donor and shallow thermal donor in silicon. *J Appl Phys* 77:943–944
- [16] Yang D, Fan R, Li L, Que D (1996) Effect of Nitrogen-Oxygen complex on electrical properties of Czochralski silicon. *Appl Phys Lett* 68:487–489
- [17] Sgourou EN, Angeletos T, Chroneos A, Lontos CA (2016) Infrared study of defects in Nitrogen-doped electron irradiated silicon. *J Mater Sci Mater Electron* 27:2054–2061
- [18] Qin Y, Wang P, Jin S, Cui C, Yang D, Yu X (2019) Effects of nitrogen doping on vacancy-oxygen complexes in neutron irradiated Czochralski silicon. *Mater Sci Semicond Processing* 98:65–69
- [19] Cui C, Ma X, Yang D (2008) Enhanced oxygen precipitation in neutron-irradiated Nitrogen -doped Czochralski Silicon crystal. *J Appl Phys* 104:123523
- [20] Stein HJ (1985) Thermal-annealing of Si-N absorption bands in nitrogen-implanted silicon. *J Electrochem Soc Solid-State Sci Technol* 132:668–670
- [21] Murphy JD, Alpass CR, Giannattasio A, Senkader S, Falster RJ, Wilshaw PR (2006) Nitrogen in silicon: transport and mechanical properties. *Nucl Inst Meth Phys Res B* 253:113–117
- [22] Kaiser W, Thurmond CD (1959) Nitrogen in silicon. *J Appl Phys* 30:427–431
- [23] Yatsurugi Y, Akiyama N, Endo Y, Nozaki T (1973) Concentration, solubility and equilibrium distribution coefficient of nitrogen and oxygen in semiconductor silicon. *J Electrochem Soc* 120:975–979
- [24] Stein HJ (1986) nitrogen in crystalline silicon. In: Mikkelsen JC Jr, Pearson SJ, Corbett JW, Pennycook SJ (eds) *Oxygen, carbon, hydrogen and nitrogen in crystalline silicon*. MRS, Pittsburgh, p 523–535
- [25] Taguchi A, Kageshima H, Wada K (2005) First – principle investigations of Nitrogen-doping effects on defect aggregation processes in Czochralski Silicon. *J Appl Phys* 97:053514
- [26.] Goss JP, Hahm I, Jones R, Briddon PR, Oberg S (2003) Vibrational modes and electronic properties of nitrogen defects in silicon. *Phys Rev B* 67:045206
- [27] Stein HJ (1983) Vibrational absorption bands for implanted Nitrogen in crystalline silicon. *Appl Phys Lett* 43:296–298
- [28] Stein HJ (1985) Infrared absorption band for substitutional nitrogen in silicon. *Appl Phys Lett* 47:1339–1341

- [29] Platonenko A, Gentile FS, Maul J, Pascale F, Kotomin EA, Dovesi R (2019) Nitrogen interstitial defects in silicon. A quantum mechanical investigation of the structural, electronic and vibrational properties. *Mater Today Commun* 21:100616
- [30] Platonenko A, Gentile FS, Pascale F, Kotomin EA, Ferrari AN, D'Amore M, Dovesi R (2019) Nitrogen substitutional defects in silicon. A quantum mechanical investigation of the structural electronic and vibrational properties. *Phys Chem Chem Phys* 21:20939
- [31] Inoue N, Kawamura Y (2018) Infrared defect dynamics – Nitrogen- Vacancy complexes in float zone grown silicon introduced by electron irradiation. *J Appl Phys* 123:185701
- [32] Karoui FS, Karoui A (2010) A density functional theory study of the atomic structure, formation energy, and vibrational properties of nitrogen-vacancy –oxygen defects in silicon. *J Appl Phys* 108:033513
- [33] Karoui A, Karoui FS, Kvit A, Rozgonyi GA, Yang D (2002) Role of nitrogen related complexes in the formation of defects in silicon. *Appl Phys Lett* 80:2114–2116
- [34] Kageshima H, Taguchi A, Wada K (2000) Theoretical investigation of Nitrogen-doping effect on vacancy aggregation processes in silicon. *Appl Phys Lett* 76:3718–3720
- [35] Voronkov VV, Falster R (2002) Intrinsic point defects and impurities in silicon crystal growth. *J Electrochem Soc* 149:G167–G174
- [36] Herzberg G, Herzberg L (1953) Rotation - Vibration spectra of diatomic and simple polyatomic molecules with long absorption paths XI. The spectrum of carbon dioxide (CO₂) below 1.25 μ . *J. Opt. Soc. Am* 43:1037–1044
- [37] Stein HJ (1988) Implanted nitrogen in germanium. *Appl Phys Lett* 52:153–154
- [38] Ganchenkova M, Supryadkina I, Abgaryan K, Bazhanov D, Mutigullin I, Borodin V (2015) Influence of ab-initio calculation parameters on prediction of energy of point defects in silicon. *Mod Electron Mater* 1:103–108
- [39] Kaukonen M, Jones R, Öberg S, Briddon PR (2001) Tin-vacancy complexes in silicon. *Phys Rev B* 64:245213
- [40.] Fukata N, Kasuya A, Suezawa M (2001) Vacancy formation energy of silicon determined by a new quenching method. *Jap J Appl Phys* 40:L854–L856
- [41] Corbett JW, Watkins GD, McDonald RS (1964) New oxygen infrared bands in annealed irradiated silicon. *Phys Rev* 135:A1381–A1385
- [42] Lee Y-H, Corbett JW (1974) EPR study of defects in neutron-irradiated silicon: Quenched-in alignment under 110-uniaxial stress. *Phys Rev B* 9:4351–4361
- [43] Brower KL (1982) Deep-level nitrogen centers in laser-annealed ion-implanted silicon. *Phys Rev B* 26:6040–6052
- [44] Sawada H, Kawakami K (2000) First-principles calculation of the interaction between nitrogen atoms and vacancies in silicon. *Phys Rev B* 62:1851–1858
- [45] Murin LI, Linström JL, Svensson BG, Markevich VP, Peaker AR, Londos CA (2005) VO_n (n \geq 3) defects in irradiated and heat-treated silicon. *Solid State Phenom* 108–109:267–272
- [46] Borghesi A, Pivac B, Sassella A, Stella A (1995) Oxygen precipitation in silicon. *J Appl Phys* 77:4169–4244
- [47] Gössele U (1986) The role of Carbon and point defects in silicon. In: Mikkelsen JC Jr, Pearton SJ, Corbett JW, Pennycook SJ (eds) Oxygen, carbon, hydrogen and nitrogen in crystalline silicon, vol 59. MRS, Pittsburgh, p 419–431
- [48] Cui C, Ma X, Yang D (2008) Enhanced oxygen precipitation in neutron-irradiated nitrogen-doped Czochralski silicon crystal. *J Appl Phys* 104:123523
- [49] Wang P, Cui C, Yu X, Yang D (2018) Growth and ripening of oxygen precipitation in neutron-irradiated Czochralski silicon. *Mat Sci Semicond Proc* 74:369–374
- [50] Watkins GD (2000) Intrinsic defects in silicon. *Mater Sci Semicond Process* 3:227–235
- [51] Londos CA, Andrianakis A, Sgourou EN, Emtsev VV, Ohyama H (2011) IR studies of the impact of Ge doping on the successive conversion of VO_n defects in Czochralski-Si containing carbon. *J Appl Phys* 109:033508
- [52] Londos CA (1985) Room-temperature irradiation of p-type Silicon. *Phys Stat Solidi (a)* 92:609–614
- [53] Bondarenko V, Krause-Rehbeig R, Feick H, Davia C (2004) Defects in FZ-Si after neutron irradiation—a positron annihilation and photoluminescence study. *J Mater Sci* 39:919–923

Publisher's Note Springer Nature remains neutral with regard to jurisdictional claims in published maps and institutional affiliations.